

Oversampled ITOF Imaging Techniques using SPAD-based Quanta Image Sensors

Neale A.W. Dutton^{1,2}, Luca Parmesan^{1,2}, Salvatore Gnecci^{1,2}, Istvan Gyongy², Neil Calder², Bruce R. Rae¹,
Lindsay A. Grant¹, Robert K. Henderson²

1 - STMicroelectronics, Imaging Division, 33 Pinkhill, EH12 7BF, Edinburgh, UK +44 131 336 6000, neale.dutton@st.com

2 - The University of Edinburgh, Edinburgh, UK

Abstract – A time-gated global shutter SPAD-based QVGA image sensor is employed as a quanta image sensor (QIS). QIS behaviour is experimentally demonstrated. Real-time temporal oversampling of time-gated binary images is implemented, facilitating two-bin indirect time of flight (ITOF) imaging with and without background rejection achieving worst case 38mm RMS precision in 600mm dynamic range.

1. INTRODUCTION

The Quanta Image Sensor (QIS) or digital film sensor is an imaging array of photo-sensitive sites with single bit output (a jot) [1][2]. Binary field images (or jot bit planes) are oversampled in either the spatial or temporal domains to form a multi-bit intensity frame image, where each pixel in the image represents a summation of jots. A single photon avalanche diode (SPAD) based QVGA QIS image sensor is presented in [3] which demonstrates real-time temporal oversampling of single photon global shutter field images. SPAD-based pixels may not scale in pitch to the 100's of nanometres regime for high spatial resolution QISs, but they have two significant advantages over photo-diode/photo-gate based CMOS image sensors (CIS): the SPAD photo detection mechanism has both picosecond temporal resolution

and single-photon sensitivity (typically 100ps RMS and >1V/ph respectively). This temporal resolution has previously been successfully demonstrated in time of flight (TOF) imaging [4]. The high sensitivity is ideal for connection to, and triggering of, a time-gated single bit memory pixel circuit [5] or a single photon counter [6]. Exploiting both these advantages, this paper proposes extending the QIS concept to a TOF binary image sensor capturing interleaved time-gated fields which are temporally oversampled to create indirect time of flight (ITOF) depth images. We propose two techniques applicable to oversampled QIS image sensors to implement two-bin ITOF imaging with and without background rejection. These are demonstrated for the first time using a time-gated SPAD-based QIS achieving 4.6x overexposure latitude in intensity and ITOF ranging with 38mm max σ in 60cm range.

2. SPAD-BASED QIS

A diagram of the global shutter SPAD-based QVGA image sensor and pixel (8 μ m, 26.8% fill factor) from [3] is shown in Fig.1 and Fig.2. Two on-chip time-gate generators are connected through two timing-balanced H-trees to row drivers. Each row input mux selects one of the two time-gate inputs. The 9T NMOS pixel has a single global shutter input from the row-wise time-gate

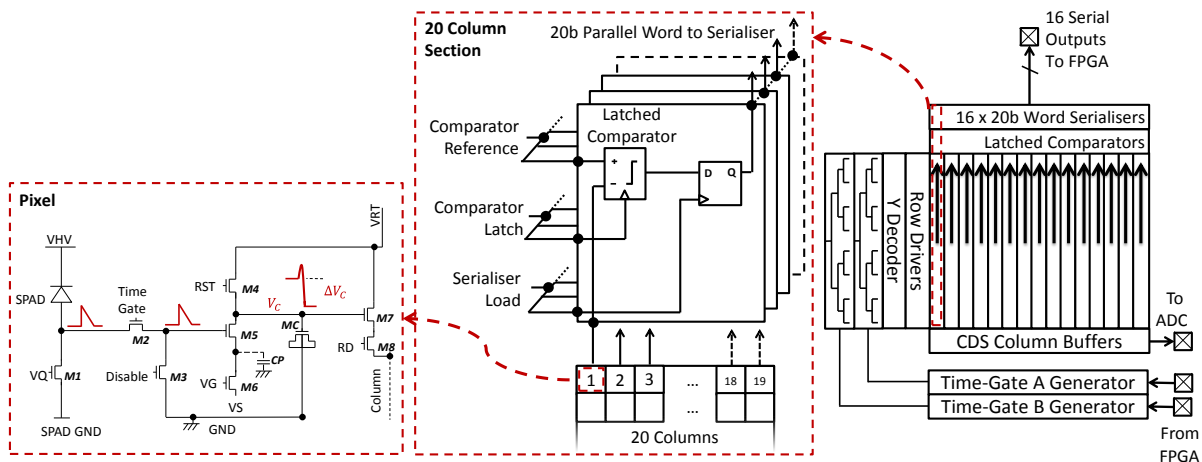


Fig. 1. Image sensor block diagram on the right with a highlighted 20-column section in the centre and pixel schematic on the left.

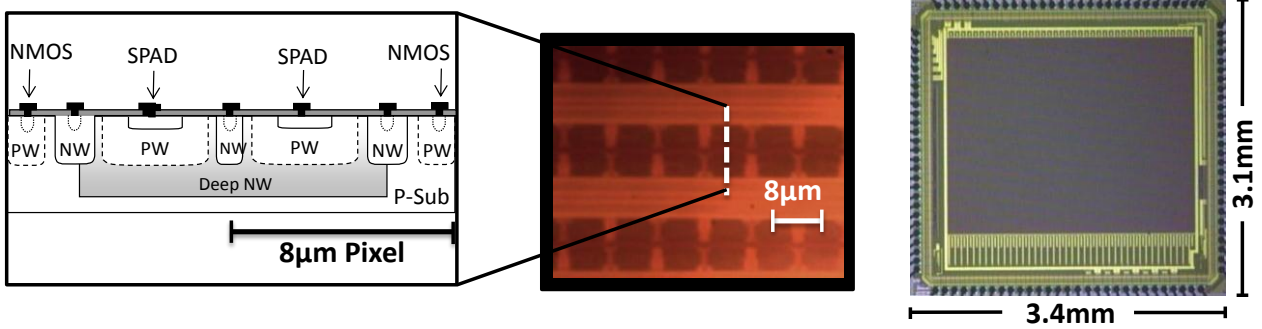


Fig. 2. Reproduced from [3]. (a) Two pixel vertical cross section. (b) Pixel array photomicrograph. (c) Sensor photomicrograph.

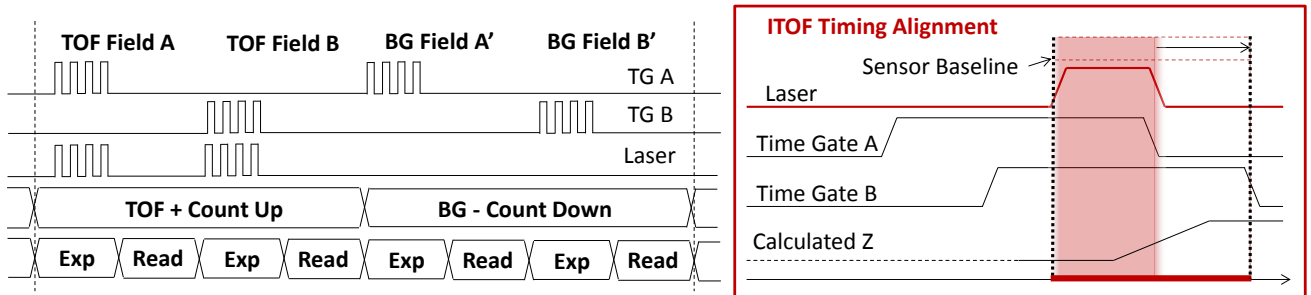


Fig. 3. System timing diagram of the 4 field ITOF capture. Temporal alignment of the laser to the time gates is shown on the right.

signal. Each pixel is biased to act as a single-bit photon-triggered dynamic memory. The column wise readout (centre of Fig.1) consists of a differential dynamic latched comparator performing a coarse flash conversion, reading out via a serialiser to an FPGA. The pixel noise mechanisms and offsets (kT/C noise, $1/f$ noise, source follower V_t variation, etc.) once input referred are rendered insignificant by the high conversion gain of the SPAD. Hence, the need for CDS is removed and the data conversion is performed in a single step.

3. ITOF IMAGING

Indirect TOF using SPAD image sensors is demonstrated with pulsed illumination in [7] and sinusoidal illumination in [4] [8]. Short nanosecond pulsed laser-diode illumination is trialled in this work. The right-hand side of Fig.3 illustrates the alignment of the illuminator pulse to the first field image time gate ('Bin A') and second field image time gate ('Bin B'). Two techniques of temporal oversampling for ITOF are trialled. The first is two interleaved fields oversampled using separate counters per pixel per field (Bin A count up and Bin B count up). Oversampling is performed off-chip on FPGA, with a RAM address for each pixel bin. The second extends this, applying the commonly used process of capturing and subtracting an ambient frame to QIS oversampling. This process is illustrated

in Fig.3, with four interleaved fields, two fields counting up with the illuminator activated (Bin A count up and Bin B count up) and subsequently two subtracting fields images with the illuminator deactivated for ambient and dark noise removal (Bin A count down then Bin B count down).

4. MEASUREMENT RESULTS

The QIS performance is measured by placing the sensor using constant illumination, incrementing the field image exposure time. The bit plane density 'D' (number of jots registering a SPAD event) is normalised, and the exposure time is normalised to quanta exposure 'H' ($3.7\mu\text{s}$ field exposure $\rightarrow 1.0H$). Fig.4 illustrates a graph of the bit density against exposure 'H', the ideal 'DlogH' QIS response from [2], and the ideal linear line are plotted alongside. Fig.5 shows the signal and noise versus exposure, highlighting at lower exposures the sensor is photon shot noise limited and at higher noise the shot noise is compressed as expected in a QIS. The overexposure latitude is calculated at $\sim 4.6x$, which again matches QIS theory. The ITOF ranging performance is characterised with the sensor and a 20mW PicoQuant FDL-500 840nm 2ns to 100ns pulse-length laser mounted on a linear motorised rail with 88% reflectance flat target. Fig.6 shows the ITOF performance of mean reported range (Z) versus rail position using a 4ns laser pulse. The standard deviation

and mean error in Z are shown in Fig.7. There is an increase in range error at low distance which is attributed to the QIS overexposure latitude which at high light level is compressing the received TOF signal and distorting the calculated range. Fig.8 presents three TOF depth images of a toy car at 30cm under the two oversampling techniques with the same scaling. In the rightmost image, the ambient subtraction is effective at retaining the original image yet the additional distance noise in the background is not fully suppressed by the thresholding algorithm.

5. CONCLUSION

A time-gated CMOS SPAD-based binary image sensor shows promising results for oversampled ITOF imaging with background rejection. Higher sensor frame rate

would improve the TOF performance by capturing additional field images per distance measurement.

References: [1] Fossum, E. "A Digital Film Sensor" in "Image Sensors and Signal Proc' for DSCs", Ed. Nakamura, J., 2005, pp 305-315
 [2] Fossum, E. R. "Modelling the Performance of Single-Bit and Multi-Bit Quanta Image Sensors". JEDS Sept. 2013. Vol.1. No.9
 [3] Dutton, N.A.W. et al "320x240 Oversampled Digital Single Photon Counting Image Sensor" VLSI Sym. 2014
 [4] Walker R. J. et al. "A 128x96 pixel event-driven phase-domain $\Delta\Sigma$ -based fully digital 3D camera in 0.13 μm CMOS imaging technology," ISSCC Tech Digest 2011.
 [5] Dutton, N.A.W. et al. "9.8 μm SPAD-based Analogue Single Photon Counting Pixel with Bias Sensitivity", IISW 2013
 [6] Pancheri, L. et al. "A 32x32 SPAD Pixel Array with Nanosecond Gating and Analog Readout" IISW 2011
 [7] Stoppa, D., et al. "A CMOS 3-D Imager Based on SPAD". TCAS I Jan. 2007. pp 4-12. Vol.54. Issue.1
 [8] Niclass, C. et al. "Single-photon synchronous detection". ESSCIRC 2008.

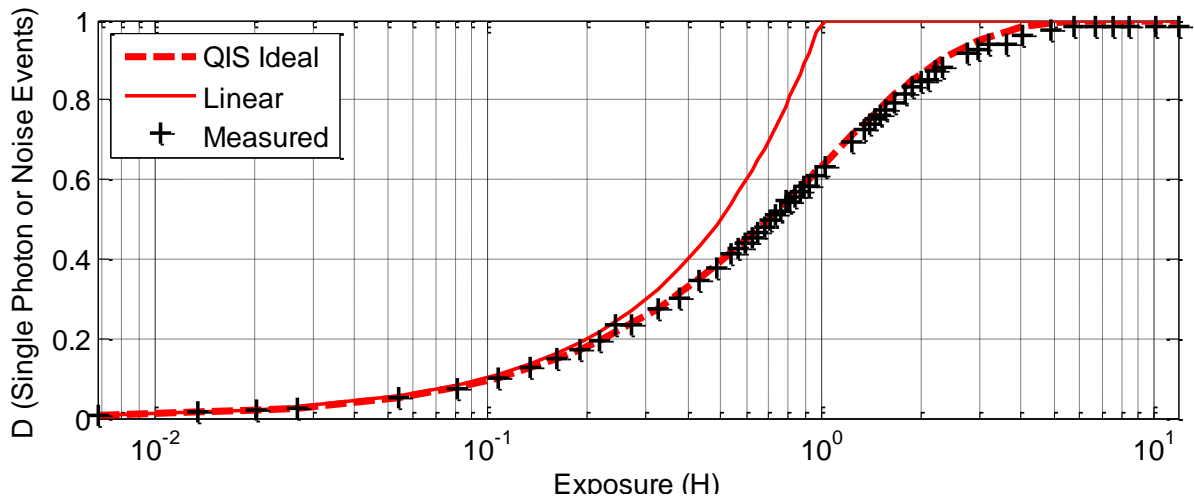


Fig. 4. D-log-H Graph: Measured field image normalised bit density 'D' versus normalised quanta exposure 'H'.

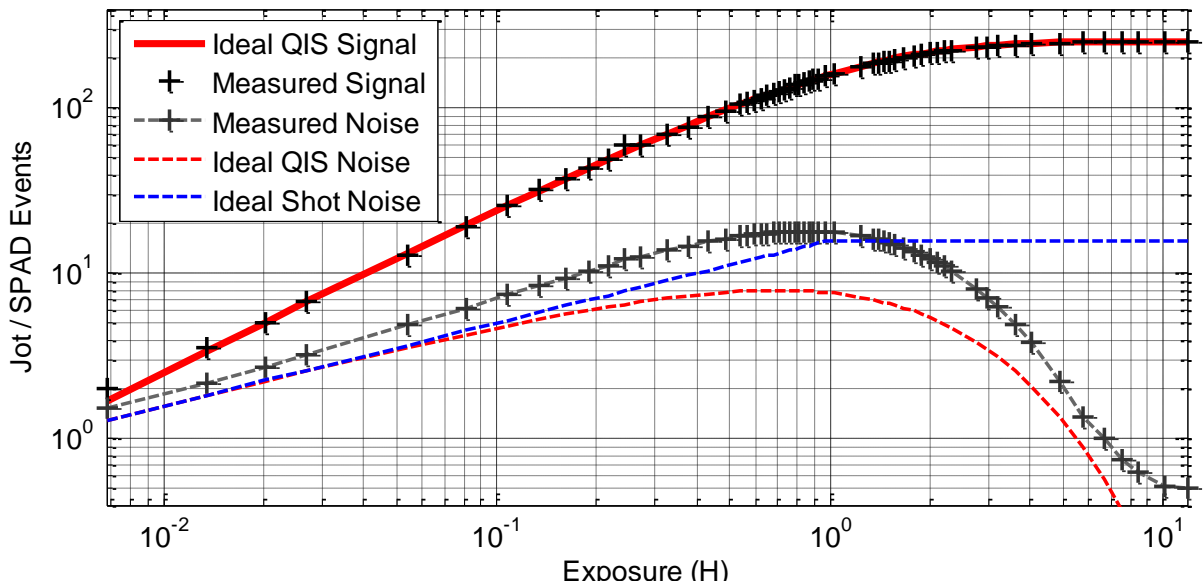


Fig. 5. Measured signal and noise versus normalized exposure of the SPAD-based QIS.

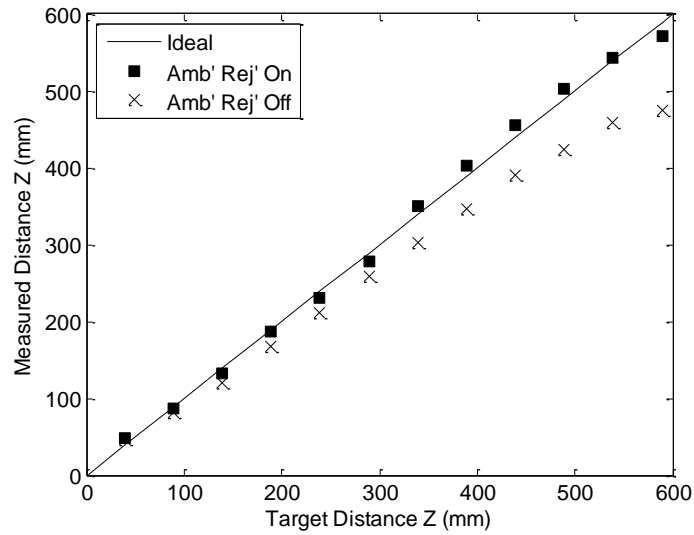


Fig. 6. TOF distance measurement for 4ns pulse width and 130k field images.

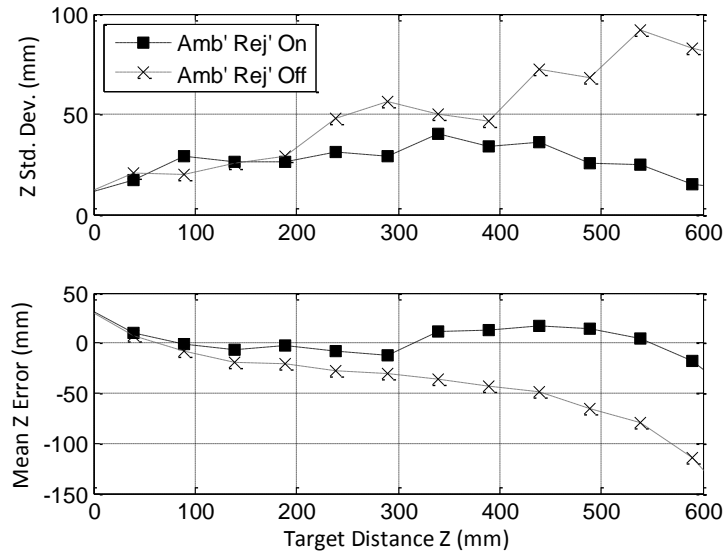


Fig. 7. Distance Std. Dev. and Mean Distance Error

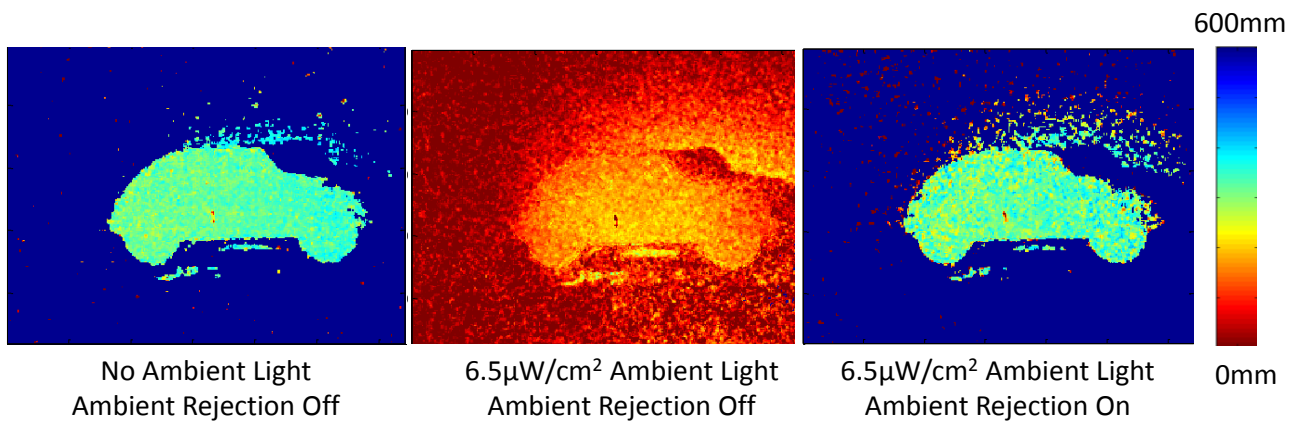


Fig. 8. TOF Images of a toy car at 30cm depth, with and without ambient rejection. Distance range is colour coded. F#2.0 lens. 20mW Illuminator. 6.5µW/cm² ambient light level at sensor (after 850nm notch filter).